Challenges of Operating Multiple Distributed Generators with Different Primary Controls Strategies in Micro-grid: Interactions and Performance Assessment

Allal El Moubarek BOUZID, Corinne Alonso, Gerard Beral

Challenges of Operating Multiple Distributed Generators with Different Primary Controls Strategies in Micro-grid: Interactions and Performance Assessment

Allal El Moubarek BOUZID · Corinne ALONSO · Gerard BERAL

Abstract This paper explores the collective efficacy of hybrid framework power-sharing control strategies within microgrid systems by integrating various droop controllers, including conventional droop, universal droop, dVOC, and VSG methodologies. Each controller's unique contributions are scrutinized concerning system stability, efficiency, and adaptability considering the impact of diverse tests on system performance. The performance analysis involves the examination of power-sharing, with a specific focus on transient and steady-state behaviors among DERs connected through complex transmission line impedances, alongside variations in local loads. The research concludes with extensive Typhoon HIL 604 real-time simulation scenarios conducted under different operating conditions, aiming to identify the optimal configuration that preserves microgrid stability.

1 Introduction

In recent years, electricity demand has surged, leading to a rise in the popularity of distributed energy resource units, particularly those based on power electronic inverters (PEI). These systems are valued for enhancing the power grid by integrating renewable energy sources (RES) and battery energy storage systems (BESS). To achieve high power levels and ensure coordinated control, multiple DERs interfaced with PEI must operate in parallel. Microgrids (MGs) have emerged as a solution, supplementing future utility grids with bidirectional power flow. However, MG operation necessitates advanced control structures to ensure efficiency, reliability, and power quality improvement across various modes of operation. [1] [2].

To solve the micro-grid problems, maintain grid stability and improve power quality while adhering to IEEE 1547 standards, the hierarchical control architecture emerged based on three levels: primary, secondary, and tertiary. Therefore, each level aims towards achieving a set of objectives while respecting the requirements of electrical standards of distribution system operators (DSO). This work concentrates on primary level control using the Droop control method, which attempts to maintain optimal power sharing between paralleled DER and local loads while maintaining electrical quantities such as voltage and frequency within permitted ranges. Literature review indicates that there are a variety approaches of droop control, classical droop control Pf & QV is frequently used. However, in microgrids with sensitive loads or voltage-sensitive loads, the Pf & QV method presents voltage regulation limitations that can lead to voltage fluctuations beyond acceptable limits. [3]. An improvement of classical droop considering current limitation was proposed in [4]. A Reverse droop control for resistive line impedance was proposed in [5], it's based on PV & Qf. However, the fixed droop slopes, like the conventional method, lack flexibility. They struggle to adapt to changing conditions, limiting the microgrid's optimization potential. A robustification technique of the conventional method was proposed in [6], it consists

A. Bouzid · G. Beral
LAAS CNRS
7 Av. du Colonel Roche, 31400 Toulouse, France
Icam site de Toulouse
75 avenue de Grande Bretagne, France
UCAC-Icam-Cameroon
Campus de Douala BP 5504 - Cameroun
e-mail: allal.bouzid@icam.fr, gerard.beral@ucac-icam.com,

C. Alonso
LAAS CNRS
Université Toulouse III , CNRS, UPS, Toulouse, France
e-mail: corinne.alonso@laas.fr

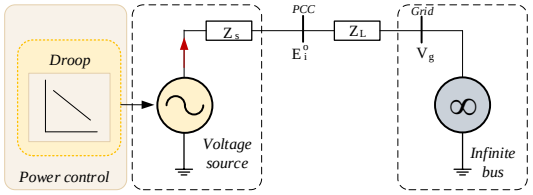

Fig. 1: Topology of a voltage source connected to an infinite bus

of improving droop architecture to work with complex impedance's [7]. An advanced droop control independent of line impedance was proposed in [8]. An adaptive droop controller was proposed in several research [9], this method is based on the estimation of all relevant parameters offering advantages in flexibility and responsiveness, but faces limitations in micro-grid applications. This method is based on the estimation of all relevant parameters offering advantages in flexibility and responsiveness and facing limitations in microgrid applications. Such as the complexity of implementing adaptive algorithms that increase system intricacy requiring meticulous parameter tuning. Additionally, they are sensitive to system changes, potentially impacting robustness and real-time performance. A virtual synchronous generator (VSG) model is proposed in [10] to improve the stability and frequency regulation within acceptable limits by incorporating the inertial characteristics of synchronous generators. VSG is an adaptive decentralized controller where each DER can operate independently to respond dynamically to fluctuations in load demand, which can enhance the scalability and adaptability and overall reliability of the micro-grid [11]. However, VSGs may exhibit transient oscillations in output power, particularly during rapid changes in load or generation. This can affect system stability and require additional control mechanisms to mitigate oscillations. Some researchers give greater interest to the dispatchable virtual oscillator control (dVOC) method [12]. It allows these DERs resources to provide grid support services such as frequency regulation, voltage regulation, and inertial response, but also achieve coordinated power sharing in demand based on the phase angle difference between its virtual oscillator and the system reference oscillator, thus enhancing the stability and reliability of the power grid. However this method presents some limitations, it may face compatibility issues with existing grid infrastructure and control systems. Integrating VOC into legacy power systems can be challenging and requires upgrades or modifications to ensure interoperability and seamless operation.

All power-sharing controllers proposed in the literature were studied alone in micro-grid and compared with other ones regarding performances and stability. Hence, this paper's principal contribution lies in investigating the performance of hybrid power-sharing control strategies in the same micro-grid system by integrating different droop controllers including conventional droop, universal droop, dVOC, and VSG methods. Combining these droop control strategies in a hybrid approach allows for synergistic benefits, compatibility study, and leveraging the strengths of each method to improve overall microgrid performance. Proposing a detailed real-time simulation of single phase micro-grid including the proposed hybrid framework for performance analysis. The analysis covers performance considerations in both transient and steady-state conditions, taking into account the impact of line impedance, and variations in load and plug & play capability. To validate the robustness of the proposed study, real-time simulations using the Typhoon HIL 604 simulator are presented.

2 Power sharing control structure of GFM

Accurate and effective power sharing among DER in microgrids ensures that each unit contributes equitably and persists in desired power-sharing steady-state distribution among all DER units. The significance of this controller is found in its ability to establish predefined use of generation units, effectively preventing overloading or under-utilization of DERs units, while ensuring stable voltage and frequency [13]. Furthermore, this can help circumvent the issue of circulating currents among DERs units within the micro-grid [14]. However, if a sudden variation of load demand or power factor results in accuracy degradation then controlling the system can become quite tricky. Crucially, this control methodology stays within the bounds of the IEEE 1547 standards, maintaining the structural integrity of the entire power system [15]. Connecting a DER unit to a microgrid requires respecting several essential connection conditions so that its synchronization with the main grid goes well. Fig. 1 illustrates the phase model of a distributed generator connected in parallel to the network via purely inductive impedance (where phase angle $\theta_g \approx \pi/2$rad) [16]. The mathematical relationships of the active and reactive powers circulating between the two energy sources can be deduced from this figure, expressed as follows:

$$P_i^o = \frac{E_i^o V_g}{Z_L}\sin(\delta),\ Q_i^o = \frac{E_i^o V_g}{Z_L}\cos(\delta) - \frac{V_g^2}{X_L} \quad (1)$$

where P_i^o and Q_i^o are the active and reactive power output of DER unit, respectively; E_i^o and V_g are the

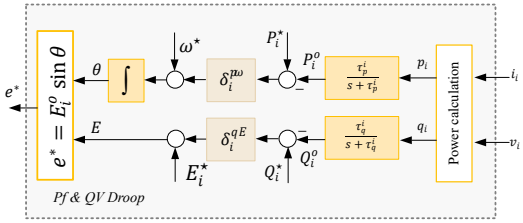

Fig. 2: Block diagram representing droop control

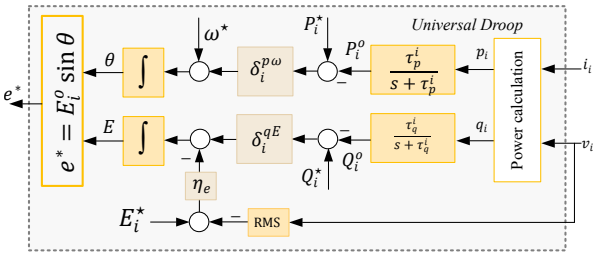

Fig. 3: Block diagram of UDC droop control

voltage amplitudes of *ith* DER unit and common point coupling (PCC), respectively; the line reactance is Z_L and δ is the power angle of the *ith* DER unit.

3 Power sharing including CDC

Conventional Droop control (CDC) concept lies on the operation of synchronous generators, which tether active and reactive powers to frequency and voltage respectively. It determines the output powers of the DER unit by considering its voltage and frequency output as the indicator as shown in Fig. 2. Thus, deviation from reference is directly correlated to the change in voltage and frequency outputs. This approach is efficient at managing power output among multiple generators, especially in situations where there are relatively small loads. However, it can be challenging to maintain accurate control and stability of the system's frequency and voltage, particularly when there are fluctuations in load demand or power factor. To reduce the crucial concerns about the power quality and satisfy the trigger limit 5% for nominal voltage $E^\star$ and 2% for nominal frequency $\omega^\star$ as stated in IEEE 1547-2018 standards [17]. Structure representation of conventional droop-controlled (CDC) DER unit is given in Fig.2. Droop control relationship based on voltage δ_i^{qE} and frequency $\delta_i^{p\omega}$ slope coefficients used to guarantee that each DER unit delivers powers according to its rated capacity is as follow :

$$\omega = \omega^\star - \delta_i^{p\omega}\left(P_i^o - P_i^\star\right) \tag{2a}$$

$$E = E^\star - \delta_i^{qE}\left(Q_i^o - Q_i^\star\right) \tag{2b}$$

The rated active power, rated reactive powers, active power output, reactive power output, nominal phase angle and voltage output for each DER unit are denoted by $P_i^\star$, $Q_i^\star$, P_i^o, Q_i^o, $\omega^\star$ and $E^\star$, respectively. The set-points are indicated by superscript $\star$.

4 Power sharing including UDC

To get universal droop control, we augment the CDC by adding an integrator in (2b) with a newly added term η_e that must be adjusted as shown in Fig. 3. η_e in (3b) multiplied by the voltage error allows for the enhancement of the transient and steady-state performances of DER unit. Through the utilization of UDC in equation (3b), direct regulation of both voltage amplitude rate of change and angular frequency is made possible.

$$\omega = \omega^\star - \delta_i^{p\omega}\left(P_i^o - P_i^\star\right) \tag{3a}$$

$$\dot{E}_i^o = \eta_e\left(E^\star - E_i^o\right) - \delta_i^{qE}\left(Q_i^o - Q_i^\star\right) \tag{3b}$$

At the steady state, the output voltage and frequency of DER unit become :

$$\omega = \omega^\star - \delta_i^{p\omega}\left(P_i^o - P_i^\star\right) \tag{4a}$$

$$E_i^o = E^\star - \frac{\delta_i^{qE}\left(Q_i^o - Q_i^\star\right)}{\eta_e E^*} E^\star \tag{4b}$$

Coefficient η_e, should be tuned carefully since they affect the dynamic response of the DER output voltage. However, voltage transient response can be accelerated by increasing the η_e coefficient.

5 Power sharing including dVOC

As proposed in [18] dVOC is a control approach based on the concept of emulating the behavior of physical oscillators [19]. When generating voltage amplitude and frequency references, dVOC takes into account the active and reactive power couplings as illustrated in Fig. 4. This section presents the mathematical model governing the behavior of virtual oscillators within the VOC framework. [20]. The differential equations used to represent the dynamics of the virtual oscillators with parameters and variables involved in the VOC model, including damping coefficients, natural frequencies, and system states in the $\alpha\beta$ coordinate space are in equation (5).

$\mathcal{R}(\zeta)$ is a rotation matrix used to perform a rotation in Euclidean space, with ζ $(0 \leq \zeta \leq \pi)$ is a parameter that allows adjusting the power-sharing controller depending on line parameters, it can take the value $\zeta = \pi/2$ for inductive lines and $\zeta = 0$ for resistive lines, $\mathcal{J} = \mathcal{R}(\pi/2)$.

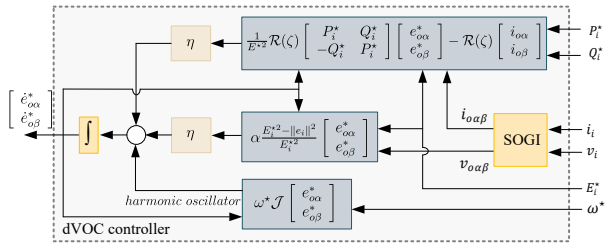

Fig. 4: Block diagram dVOC control

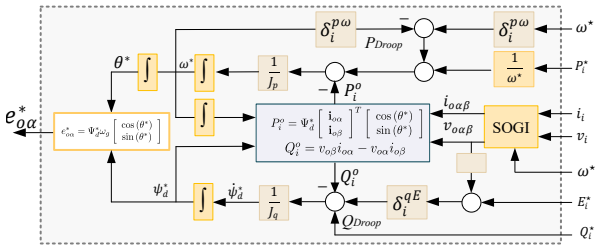

Fig. 5: Block diagram of VSG droop control

$$\theta_{vsm} = \omega^\star + \arctan\left(\frac{e^*_{o\beta}}{e^*_{o\alpha}}\right) \tag{6}$$

$$\mathcal{R}(\zeta) := \begin{bmatrix} \cos(\zeta) & -\sin(\zeta) \\ \sin(\zeta) & \cos(\zeta) \end{bmatrix}$$

The quantities $\eta > 0, \alpha > 0$. From the dVOC droop law (5), we can define the droop coefficients for voltage $\delta_i^{qE} = 1/\alpha E^\star$ and frequency $\delta_i^{p\omega} = \eta/E^{\star 2}$. The equation of voltage angle calculation is presented in (6). The schematic of dVOC control is shown in Fig. 4.

6 Power sharing including VSG

This section outlines the mathematical modeling used to describe the behavior of VSGs within microgrid systems, including equations characterizing the dynamics related to power output, voltage regulation, and inertial response. The active and reactive power control laws of the virtual synchronous generator can be written as :

$$\begin{aligned} \dot{\omega}^* &= \frac{1}{J_p}\left(\overbrace{\delta_i^{p\omega}\left(\omega^\star - \omega^*\right)}^{P_{droop}} + \frac{P_i^\star}{\omega^\star} - \overbrace{\Psi_d^* \begin{bmatrix} \mathbf{i}_{o\alpha} \\ \mathbf{i}_{o\beta} \end{bmatrix}^T \begin{bmatrix} \cos(\theta^*) \\ \sin(\theta^*) \end{bmatrix}}^{P_i^o}\right) \\ \dot{\Psi}_d^* &= \frac{1}{J_q}\left(\overbrace{\delta_i^{qE}\left(E^\star - E_i^o\right)}^{Q_{droop}} + Q_i^\star - \overbrace{v_{o\beta} i_{o\alpha} - v_{o\alpha} i_{o\beta}}^{Q_i^o}\right) \end{aligned} \tag{7}$$

where $J_{p,q}$ is the virtual moment of rotational inertia and damping coefficient; $P_i^\star$ and P_i^o are the mechanical applied to the rotor (prime mover power in a SG with $P_i^\star = T_m\omega^\star$) and electromagnetic powers (electric output power of VSG: $P_i^o = T_e/\omega^*$ with T_e is the electromagnetic torque), respectively; ω^* and ω are the mechanical virtual angular frequency and actual angular frequency of the grid, respectively. In the case of a standalone microgrid, ω is considered as the reference of the angular grid frequency. The VSG generated voltage amplitude is from reactive power control loop Eq (7) as follows:

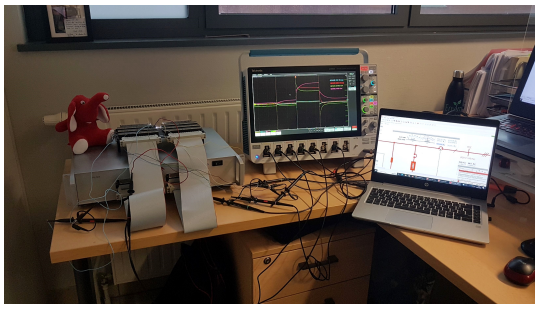

Fig. 6: Implementation Typhoon-HIL 604 block diagram and real-time simulation setup

$$e^*_{o\alpha} = \Psi_d^* \omega_g \begin{bmatrix} \cos(\theta^*) \\ \sin(\theta^*) \end{bmatrix} \tag{8}$$

7 Simulation result analysis

To verify the effectiveness and reliability of the parallel DER units in single-phase standalone AC microgrids under different droop controllers combination typologies, a real-time simulation and analysis are conducted under various scenarios. The implementation is carried out using Typhoon HIL604 real-time simulator as shown in Fig. 6. The interface between the real-time digital simulator HIL 604, I/O interface cards, and Typhoon schematic is provided by Control Center software version 2024.1. Results are taken in the MSO of the TEKTRONIX 5 series (6.25 GS/s, 350 Mhz).

7.1 Transient and steady-state performances

The single-phase AC microgrid structure is shown in Fig. 7. Five multi-DERs units are connected in parallel (in the standalone mode) for power sharing common loads (resistive (R) 33kVA and resistive inductive

$$\begin{bmatrix} \dot{e}^*_{o\alpha} \\ \dot{e}^*_{o\beta} \end{bmatrix} = \overbrace{\omega^\star \mathcal{J} \begin{bmatrix} e^*_{o\alpha} \\ e^*_{o\beta} \end{bmatrix}}^{harmonic\ oscillator} + \eta \left(\overbrace{\frac{1}{E^{\star 2}} \mathcal{R}(\zeta) \begin{bmatrix} P_i^\star & Q_i^\star \\ -Q_i^\star & P_i^\star \end{bmatrix} \begin{bmatrix} e^*_{o\alpha} \\ e^*_{o\beta} \end{bmatrix} - \mathcal{R}(\zeta) \begin{bmatrix} i_{o\alpha} \\ i_{o\beta} \end{bmatrix}}^{phase\ error\ term} + \alpha \overbrace{\frac{E_i^{\star 2} - \|e_i\|^2}{E_i^{\star 2}} \begin{bmatrix} e^*_{o\alpha} \\ e^*_{o\beta} \end{bmatrix}}^{magnitude\ error\ term} \right) \tag{5}$$

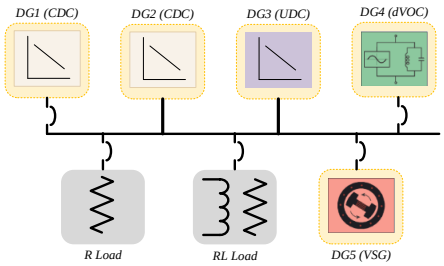

Fig. 7: Single phase micro-grid structure setup

(RL) 33kVA at 0.7 Lagging Power Factor), the different primary power sharing control configuration is used to control DER units. The two first DER units ($N1$ and $N2$) employ a CDC method, the UDC is implemented in DER unit $N3$. Advanced power-sharing controllers based on dVOC and VSG are implemented in DER units $N4$ and $N5$, respectively. The objective of this test is to verify the behavior of different power-sharing controllers supplying together a common load in the same network.

Fig. 8 show the transient and steady-state performance of the studied system, we can observe that all primary controllers remain stable at steady-state for all electrical quantities (active and reactive power, voltage, current, and frequency). However, we can observe that UDC controller creates a little high drop voltage compared with the other controllers caused by the supplementary control mechanism based on the integral action in the voltage loop. So, to avoid this problem, it's necessary to carefully design the coefficient η_e based on operating conditions without causing of instability in the system. However, we can observe that the power-sharing controllers unevenly distribute the required power demand among DERs when the load increases. The problem stems from the droop characteristic, which can result in variations in power output. So, generators with steeper droop slopes may boost their power output faster compared to those with shallower slopes. This involves the use of a secondary level controller to ensure reactive powers alignment. In terms of transient performance, the analysis indicates a fast transient with overshoot regarding the dVOC method compared to other controllers, although all remain within acceptable limits. However, VSG responds slowly to sudden load fluctuations or disturbances due to providing inertia and damping characteristics.

Table 1: Micro-grid parameters for real-time simulation

Parameter	**Value**
Apparent power	S = 33 kVA
Grid voltage	$V = 220V_{RMS}$
Grid frequency	$f = 60Hz$
Upper margin Step-time	$T_s = 50e-6s$
Switching frequency	$f_s = 10kHz$
DC link voltage	$V_{dc} = 1500V$
DG side inductance	$L_f = 25e-3mH$
DG side capacitance	$C_f = 100\mu F$
CDC Coefficients	$\delta_i^{p\omega} = 5.71e^{-4}$; $\delta_i^{qE} = 6.67e^{-4}$
UDC Coefficients	$\delta_i^{p\omega} = 5.71e^{-4}$; $\delta_i^{qE} = 6.67e^{-4}$ $\eta_e = 0.015$
dVOC coefficients	$\eta = 55$ $\alpha = 1.6$
VSG Coefficients	$\delta_i^{p\omega} = 29$ $\delta_i^{qE} = 1.5e^3$ $J_p = 2.9$ $J_q = 42.5e^3$

7.2 Plug & play DER units

In this section, load variation scenarios, coupled with plug-and-play tests for DER units within a micro-grid system, are meticulously evaluated to confirm the adaptability and stability of mixed power-sharing controllers. Based on Fig. 9 and Fig. 10, variation scenarios are as follow : At start all DER units are connected with initial AC load1 (16.5 kW) followed by $t1$ where DER1 is disconnected. At $t2$, AC load2 (16.5kW +j11.55kVAR) is connected and disconnected at $t3$, followed by disconnection of DER4 and DER5 at $t4$ and $t5$, respectively. We can observe that load variations involve all DER units in increasing or decreasing power sharing, and the system remains stable. The disconnection of DER1, followed by DER4 and DER5 respectively while the micro-grid is operational, enables other units to conform to this updated configuration, ensuring the uninterrupted provision of service. This approach avoids any disturbance to ongoing operations and maintains system stability with effective power sharing during these transitions.

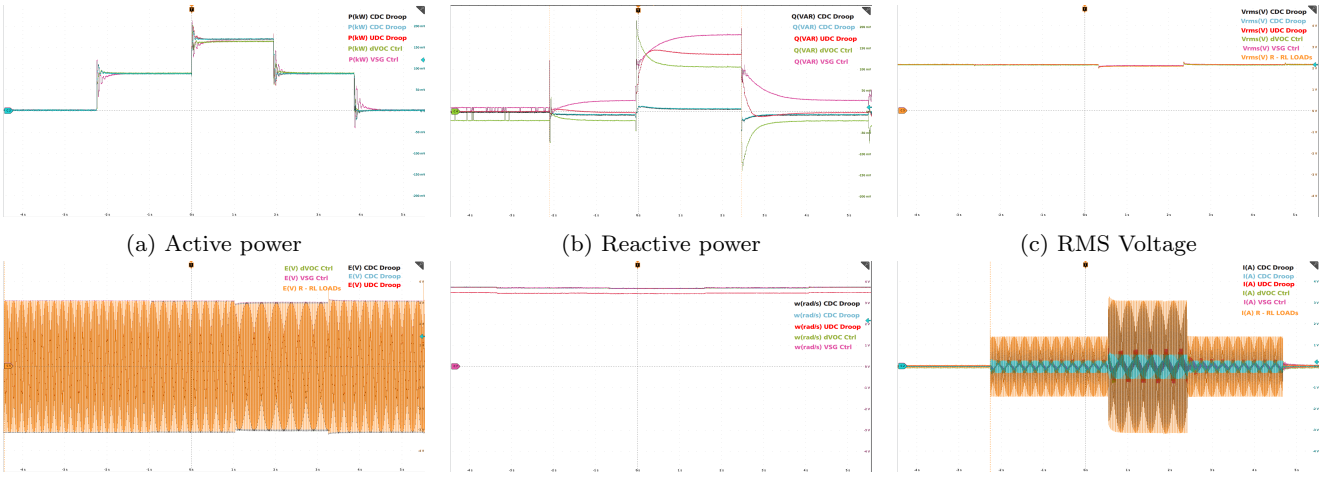

(a) Active power (b) Reactive power (c) RMS Voltage

(d) Single phase voltage (e) Frequency (f) Single phase current

Fig. 8: Standalone AC micro-grid simulation results under power sharing among resistive and resistive inductive loads

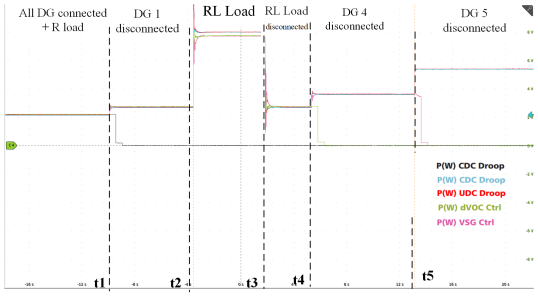

Fig. 9: Active power result under DER units disconnection

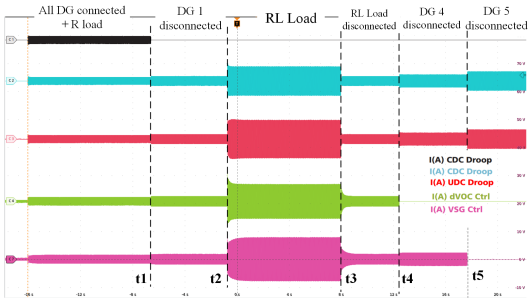

Fig. 10: Phase current result under DER units disconnection

8 Conclusions

This paper integrates a hybrid framework for power sharing control in a single-phase AC microgrid to evaluate system performance and stability during common load supply and DER disconnection. Controllers ensure stability at steady-state, effectively sharing active power in proportion to the load, with a particular focus on dVOC and VSG control. These controllers maintain stable operation and respond well to system transients, critical for reliable operation. The novelty in this article is the combination of conventional and universal droop control with dVOC and VSG power-sharing strategies into a hybrid framework, the micro-grid benefits from their complementary strengths. The integration of controllers synergistically enhances system resilience, load power sharing, and grid support capabilities, ultimately fostering efficient and reliable microgrid operations. Future work aims to evaluate these methods in larger microgrids with complex configurations, expanding test scenarios with time and frequency analysis.

References

1. R. Lasseter, A. Akhil, C. Marnay, J. Stevens, J. Dagle, R. Guttromson, S. A. Meliopoulous, R. Yinger, and J. Eto, "The certs microgrid concept, white paper on integration of distributed energy resources," *California Energy Commission, Office of Power Technologies-US Department of Energy, LBNL-50829, http://certs. lbl. gov*, 2002.
2. D. E. Olivares, C. A. Cañizares, and M. Kazerani, "A centralized energy management system for isolated microgrids," *IEEE Transactions on smart grid*, vol. 5, no. 4, pp. 1864–1875, 2014.
3. S. Mohammad Tayyeb and R. Krishan, "Data-centric decentralised controller for effective p-f and q-v control in ac microgrids," in *2023 IEEE 3rd International Conference on Sustainable Energy and Future Electric Transportation (SEFET)*, pp. 1–6, 2023.
4. L. Huang, H. Xin, Z. Wang, L. Zhang, K. Wu, and J. Hu, "Transient stability analysis and control design of droop-controlled voltage source converters considering current

limitation," *IEEE Transactions on Smart Grid*, vol. 10, no. 1, pp. 578–591, 2017.
5. Y. Han, H. Li, P. Shen, E. A. A. Coelho, and J. M. Guerrero, "Review of active and reactive power sharing strategies in hierarchical controlled microgrids," *IEEE Transactions on Power Electronics*, vol. 32, no. 3, pp. 2427–2451, 2016.
6. Q.-C. Zhong and Y. Zeng, "Universal droop control of inverters with different types of output impedance," *IEEE Access*, vol. 4, pp. 702–712, 2016.
7. M. Amin and Q.-C. Zhong, "Resynchronization of distributed generation based on the universal droop controller for seamless transfer between operation modes," *IEEE Transactions on Industrial Electronics*, vol. 67, no. 9, pp. 7574–7582, 2019.
8. D. Govind, H. M. Suryawanshi, P. Nachankar, C. L. Narayana, and A. Singhal, "A modified voltage controller with advanced droop control for load sharing in standalone ac microgrid under different load conditions," *IEEE Transactions on Industry Applications*, 2023.
9. C. Gómez-Aleixandre, Á. Navarro-Rodríguez, M. Langwasser, P. García, and M. Liserre, "Weighted dc virtual generator control scheme for interlinking converters in dc microgrids," *IEEE Transactions on Industrial Electronics*, 2023.
10. J. Wang and X. Zhang, "Transient virtual inertia optimization strategy for virtual synchronous generator based on equilibrium point state assessment," *International Journal of Electrical Power & Energy Systems*, vol. 155, p. 109588, 2024.
11. Q. Zhong, "Reconfiguration of inertia, damping and fault ride-through for a virtual synchronous machine," Apr. 7 2020. US Patent 10,615,716.
12. X. He, V. Häberle, and F. Dörfler, "Complex-frequency synchronization of converter-based power systems," 2022.
13. F. Katiraei, R. Iravani, N. Hatziargyriou, and A. Dimeas, "Microgrids management," *IEEE power and energy magazine*, vol. 6, no. 3, pp. 54–65, 2008.
14. J. M. Guerrero, M. Chandorkar, T.-L. Lee, and P. C. Loh, "Advanced control architectures for intelligent microgrids—part i: Decentralized and hierarchical control," *IEEE Transactions on Industrial Electronics*, vol. 60, no. 4, pp. 1254–1262, 2012.
15. T. Basso, S. Chakraborty, A. Hoke, and M. Coddington, "Ieee 1547 standards advancing grid modernization," in *2015 IEEE 42nd photovoltaic specialist conference (PVSC)*, pp. 1–5, IEEE, 2015.
16. Z. Gao, W. Du, and H. Wang, "Transient stability analysis of a grid-connected type-4 wind turbine with grid-forming control during the fault," *International Journal of Electrical Power & Energy Systems*, vol. 155, p. 109514, 2024.
17. "Ieee standard for interconnection and interoperability of distributed energy resources with associated electric power systems interfaces," *IEEE Std 1547-2018 (Revision of IEEE Std 1547-2003)*, pp. 1–138, 2018.
18. D. Groß, M. Colombino, J.-S. Brouillon, and F. Dörfler, "The effect of transmission-line dynamics on grid-forming dispatchable virtual oscillator control," *IEEE Transactions on Control of Network Systems*, vol. 6, no. 3, pp. 1148–1160, 2019.
19. B. B. Johnson, S. V. Dhople, A. O. Hamadeh, and P. T. Krein, "Synchronization of parallel single-phase inverters with virtual oscillator control," *IEEE Transactions on Power Electronics*, vol. 29, no. 11, pp. 6124–6138, 2013.
20. G.-S. Seo, M. Colombino, I. Subotic, B. Johnson, D. Groß, and F. Dörfler, "Dispatchable virtual oscillator control for decentralized inverter-dominated power systems: Analysis and experiments," in *2019 IEEE Applied Power Electronics Conference and Exposition (APEC)*, pp. 561–566, IEEE, 2019.